18èmes Journées Internationales de Thermique (JITH 2017)
Monastir (Tunisie), 25 - 27 Octobre 2017

Two Dimensional Modeling of Heat and Mass Transfer of Deformable Media during Convective Drying Process

Imène HERMASSI, Lamine HASSINI, Soufien AZZOUZ, Ali BELGHITH

Laboratoire d'Energétique et des Transferts Thermique et Massique (LETTM). Département de Physique.
Faculté des Sciences de Tunis. Université de Tunis El Manar. Tunis. Tunisia
imenhermassi@yahoo.fr

Résumé : The objective of the present work is the understanding and simulating in two-dimensions the spatio-temporel variation of the moisture content, temperature and mechanical stress behaviour for seedless grape along convective drying. Assuming that our sample was viscolelastic, shrinkage was isotropic and the deformation was plane, we were developed a hydro-thermal model incorporated with a mechanical model. The model was adopted to represent the drying behaviour of seedless grape under several operating conditions, taking into consideration the variation of the properties of the sample during drying process.

Mots clés : Convective Drying, Seedless Grape, Modeling, Relaxation Test, Viscoelastic Stress.

1. Introduction

Drying is an important operation in many productions and treatment processes, its importance come down to its facility and it stay always the common method to preserve a variety of food products. For food sector drying is used as a way of preservation which is important for the safety, the stability and the reliability of the product, since it decreases the water activity of the product, reduces microbiological activity and minimizes physical and chemical changes during storage [1]. Actually, the quality of dried products is in great requiring worldwide. The preservation of the quality of dried products is a major interest Therefore, we should predict the damaging and cracking of these products undergoing drying process, a large variety of models has been developed for simulate and modeling the drying phenomena with different approaches [2], [3], [4]. There are different formulations for the dynamic analysis of spatial mechanisms which vary in the system of coordinates used and in the way they introduce mathematical equations. The moisture loss during grape drying inevitably introduces variation in the material dimensions due to shrinkage. When the stress becomes significantly large through the grape berry body, this leads to some large deformations and, above certain limits, to damage, like cracks and important energy consumption. Consequently, it is interesting to describe mathematically the drying process in order to optimize and control all the mechanisms involved in the drying process. The quality of the product has to bring many concepts such as nutritional control, microbiological safety and sensorial characteristics [5]. As for grape, all the rheological properties can be related to temperature and moisture content of the sample. Moreover mathematical modeling allows the manufacturers to strongly push the design of new products and processes. In fact, the use of simulative tools opens new ideas without incurring the usual high research costs linked to pilot investigations.

The main objective of the present work is to formulate an accurate transport model analyzing the simultaneous transfers of heat and mass within grape. The suggested model takes into account grape deformation and allows determine the time and space evolutions of moisture content, temperature and solid displacement within grape.

1. Mathematical model

2.1. Assumptions

The studied sample is presented in Figure 1. The grape berry is a spherically shaped product, it was exposed to an air-vapor mixture with controlled air conditions (air velocity, air temperature and relative humidity).

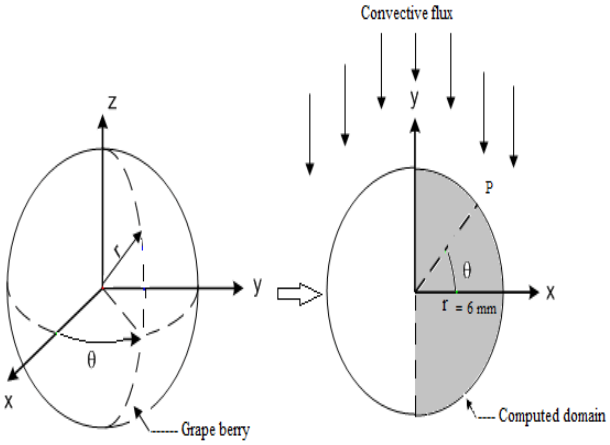

Figure 1: Geometrical configuration of the product and the computational domain.

Several simplifying assumptions were made in order to obtain the mathematical model equations:

- The grape is supposed spherical with an axis- symmetry;
- The product is biphasic water-solid;
- Initially the moisture and the temperature of the grape are uniform;
- The stress has no reciprocal influence on heat and moisture transfers;
- Heat and mass transfers are governed by diffusion within the product and by convection between the material and the environment air;
- The boundary conditions for the moisture and the temperature transfers stimulate the symmetry of the moisture and temperature potentials at the middle point of the berry grape;
- The shrinkage was ideal and isotropic;
- The material behaved according to the generalized Maxwell viscoelasticity model with five elements.

2.2. Mass Conservation Equations

The conservation equations of the solid and water phases are written respectively:

Solid: $$\frac{\partial c_s}{\partial t} = -div(c_s u_s) \qquad (1)$$

Liquid: $$\frac{\partial c_l}{\partial t} = -div(c_l u_l) \qquad (2)$$

The internal mass transfer which was considered to be governed by Fick's law, with a moisture diffusivity coefficient D, is described by the following equation as follows:

$$\frac{1}{1+\beta X}\frac{\partial X}{\partial t} = \frac{1}{r^2}\frac{\partial}{\partial r}\left(\frac{r^2 D}{1+\beta X}\frac{\partial X}{\partial r}\right) + \frac{\partial}{\partial z}\left(\frac{D}{1+\beta X}\frac{\partial X}{\partial z}\right) - \frac{u_s^r}{1+\beta X}\frac{\partial X}{\partial r} - \frac{u_s^z}{1+\beta X}\frac{\partial X}{\partial z} \qquad (3)$$

2.3. Energy Conservation Equations

According to the assumption that the evaporation occurs only at the surface level of the product, the internal heat transfer obeys to the Fourier's law with an apparent conductivity coefficient depending on the moisture content and could be expressed as follows:

$$\frac{\rho_s}{1+\beta X}\left(C_{ps}+XC_{pl}\right)\frac{\partial T}{\partial t}=\frac{1}{r^2}\frac{\partial}{\partial r}\left(r^2\lambda\frac{\partial T}{\partial r}\right)+\frac{\partial}{\partial z}\left(\lambda\frac{\partial T}{\partial z}\right)-\frac{\rho_s}{1+\beta X}\left(C_{ps}+XC_{pl}\right)u_s^r\frac{\partial T}{\partial r}-\frac{\rho_s}{1+\beta X}\left(C_{ps}+XC_{pl}\right)u_s^z\frac{\partial T}{\partial z} \quad (4)$$

2.4. Structural Mechanics Equations

Many research used the mechanical model which consisted mainly of the mechanical equilibrium equation Eq. (5) and the viscoelastic behavior equation Eq. (6) as developed by [6]:

$$\Delta\left(\sigma_{ij}\right)=0 \quad (5)$$

$$\sigma_{ij}\int_0^t\left[K\left(t-\tau,X\right)-\frac{2}{3}G\left(t-\tau,X\right)\right]\frac{\partial\varepsilon_{ij}^m\left(\tau\right)}{\partial\tau}\delta_{ij}d\tau+2\int_0^t G\left(t-\tau,X\right)\frac{\partial\varepsilon_{ij}^m\left(\tau\right)}{\partial\tau}d\tau \quad (6)$$

where K is the bulk modulus and G is the shear and expressed respectively as:

$$K\left(t,X\right)=\frac{E\left(t,X\right)}{2\left(1+\upsilon\right)} \quad (7)$$

$$G\left(t,X\right)=\frac{E\left(t,X\right)}{3\left(1-2\upsilon\right)} \quad (8)$$

E (t, X) is the relaxation modulus, determined experimentally, υ is the Poisson's ratio, t is the current drying time, and δ_{ij} is the Kronecker's delta.

ε_{ij} is the local strain, it is the sum of the mechanical strain ε_{ij}^m and the hydric strain ε_{ij}^h, expressed as follows [7], [8]::

$$\varepsilon_{ij}=\varepsilon_{ij}^m+\varepsilon_{ij}^h \quad (9)$$

with:

$$\varepsilon_{ij}^h=\alpha\left(X-X_0\right)\delta_{ij} \quad (10)$$

In numerical solid mechanics, these equations are solved in terms of displacements (u).
The relations between the elements of the total strain tensor, displacements, and solid matter velocity with the assumption of a small deformation (second order effects assumed to be negligible) are given below:

$$\varepsilon_{rr}=\frac{\partial u_r}{\partial r} \quad (11)$$

$$\varepsilon_{zz}=\frac{1}{r}\left(\frac{\partial u_z}{\partial z}+u_r\right) \quad (12)$$

$$u_s^i=\frac{\partial u_i}{\partial t} \quad (13)$$

2.5. Initial and boundary conditions

Initial and boundary conditions are expressed as follows:
Initially, the temperature and moisture content of the material are uniform:

$$t=0;X=X_0;T=T_0;\sigma_{ij}=0 \quad (14)$$

The following boundary conditions were applied (t>0):
The heat and water transfer at the sample top and side external surface (in contact with air) was supposed to be purely convective:

$$\frac{\rho_s}{1+\beta X}\left(-D\frac{\partial X}{\partial n}+Xu_s^n\right)=k\frac{P_{atm}M_v}{RT_a}Ln\left(\frac{P_{atm}-RHP_{vsat}\left(T_a\right)}{P_{atm}-a_w\left(X,T\right)P_{vsat}\left(T\right)}\right) \quad (15)$$

$$-\lambda\frac{\partial T}{\partial n}+\frac{\rho_s}{1+\beta X}\left(C_{ps}+XC_{pl}\right)Tu_s^n-K\frac{P_{atm}M_v}{RT_a}Ln\left(\frac{P_{atm}-RHP_{vsat}\left(T_a\right)}{P_{atm}-a_w\left(X,T\right)P_{vsat}\left(T\right)}\right)L_{vap}=h\left(T-T_a\right)\qquad(16)$$

where n denotes the space coordinate at which the axis is normal to the considered surface, u_s^n is the solid velocity normal to that surface, P_{vsat} is the saturated vapor pressure, RH is the air relative humidity, a_w is the water activity within the product, λ is the product thermal conductivity, L_{vap} is the latent heat of water vaporization, C_p is the specific heat (l for liquid, s for solid), k is the convective mass transfer coefficient, and h is the convective heat transfer coefficient.

At any point of the product's external surface, the stress that is normal to that surface is zero [7]:

$$\sigma_{ij}^{surf}=0\qquad(17)$$

The heat and mass transfer and the solid displacement in the θ direction at the surface in contact with the shelf (Z = 0) were as follows:

$$\frac{\partial X}{\partial Z}=0;\quad\frac{\partial T}{\partial Z}=0;\quad u_Z=0\qquad(18)$$

The heat and mass transfer and the solid displacement in the r (radial) direction at the symmetry plane (r = 0) were considered nil:

$$\frac{\partial X}{\partial r}=0;\quad\frac{\partial T}{\partial r}=0;\quad u_r=0\qquad(19)$$

The values or expressions (functions of X and T) for all material thermophysical properties (water diffusivity D, heat conductivity λ, heat specific capacity C_p, water activity a_w) and external heat and mass transfer coefficients (h and k) needed for simulations are given in Table 1.

Table1: Seedless grape properties and external heat and mass transfer coefficients

Property	**Value or correlation**				**Reference**
Specific heat capacity of liquid water	$C_{pl}=4182\left(J.kg^{-1}.K^{-1}\right)$				[9]
Specific heat capacity of solid matter	$C_{ps}=1254\left(J.kg^{-1}.K^{-1}\right)$				[9]
Hydric diffusivity	$D(X,T)=8.48\times10^{-2}\exp\left(-\frac{57.56}{RT}\right)\exp\left(\left(0.01T-4.149\right)X\right)\left(m^2.s^{-1}\right)$				[10]
Latent heat of water vaporization	$L_{vap}=4186\left(597-0.56T\right)\left(J.kg^{-1}\right)$				[9]
Equilibrium moisture content(GAB Model)	$X_{eq}\left(a_w,T\right)=\frac{X_mCKa_w}{\left(1-Ka_w\right)\left(1-Ka_w+CKa_w\right)}\left(kg^{-1}.kg^{-1}\right)$				[10]
	T(°C)	**X_m ($kg^{-1}.kg^{-1}$)**	**K**	**C**	
	70	11.337	0.865	0.101	
Volumetric hydro-contraction coefficient dry basis	$\beta=1.315$				[10]
Thermal conductivity	$\lambda(X)=\frac{0.069+0.473X}{1+X}\left(W.m^{-2}.K^{-1}\right)$				[9]
Poisson's ratio	$\upsilon=0.49$				[11]
Density of dry solid	$\rho_s=1379\left(kg.m^{-3}\right)$				[10]

Convective heat transfer coefficient	$h=\frac{\lambda_a}{d}\left[2+\left(0.4Re^{0.5}+0.06Re^{0.67}\right)Pr^{0.4}\right]\left(W.m^{-2}.K^{-1}\right)$	[11]
Convective mass transfer coefficient	$K=\frac{D}{d}\left[2+\left(0.4R_e^{0.5}+0.06R_e^{0.0.67}\right)Sc^{0.4}\right]\left(m.s^{-1}\right)$	[11]

2.6. Model Implementation

The coupled heat and mass transfer equations, and mechanical equilibrium equations, along with the viscoelastic rheological behavior law, were solved simultaneously on a variable geometrical domain. In that way, and unlike in some other works on this subject, the actual deformation of the sample respecting the global equilibrium and boundary constraints, and not an arbitrary one, was applied to solve the heat and mass balances. Because of the symmetry of the problem (Figure 1), the model equations were solved on a two-dimensional domain. The governing equations, as well as initial and boundary conditions, were numerically implemented by means of the COMSOL Multiphysics finite-element software (version 3.5a) using both the Chemical Engineering and the Structural Mechanics modules and moving mesh application mode. The computational mesh to map the solution domain was defined by means of triangular elements. Different mesh sizes were tested to ensure the mesh-independent numerical results [1].

2.7. Elastic and Shear Modulus

The grape viscoelastic properties was determined using a traction-compression machine LLOYDAMETEK TA1S (Figure 2), consisting essentially of a mono-column force sensor with a capacity of 250N sliding on the column and a support for maintaining the studied sample. Compression tests are controlled by a data analysis software which allows also to record data on a microcomputer and to provide calculated results from the readings of Force / strain or stress / strain.

Figure 2: Tensile and Compression Strength- machine.

During a stress relaxation experiment, a constant deformation (strain) is instantaneously applied to the sample, and the resulting force (stress) is recorded as a function of time. Spherical fresh grape samples (r = 6 mm), conditioned previously at different moisture contents, were kept at the constant compressive strain of 3% (by applying a load of 10 N) for about 30 min. All experiments were performed at room temperature of 25°C. The tests were replicated three times. The measured instant stress was converted to an instant modulus, E, by dividing the latter by the constant strain. Experimental relaxation curves for different moisture contents are shown in Figure 3.

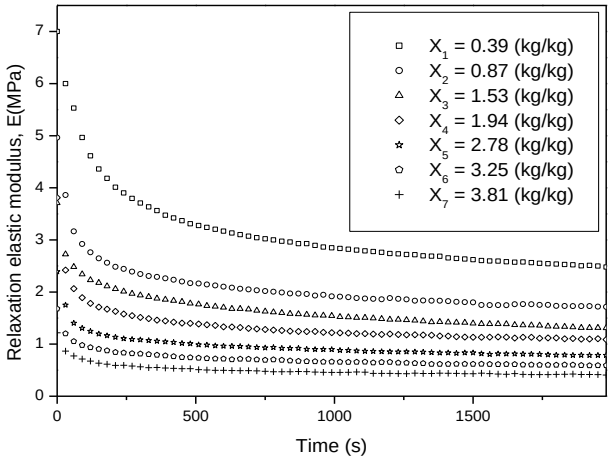

Figure 3: Relaxation elastic modulus versus time at different moisture contents.

The relaxation behavior of grape was best described by a five-parameter Maxwell model, consisting of two spring-dashpot branches and one spring branch representing the elastic modulus (E_c) at infinite time [12], [13]. In the present work, we were considering the model parameters as a function of the moisture content X. The evolution of the modulus E with time was thus expressed as:

$$E(X,t) = E_c(X) + E_1(X)\exp\left(-\frac{t}{\tau_1}\right) + E_2(X)\exp\left(-\frac{t}{\tau_2}\right) \qquad (21)$$

where E_1 and E_2 are the elastic modulus for each Maxwell branch, and τ_1 and τ_2 are the corresponding relaxation times. At a given moisture content, the values of these parameters are determined by fitting the corresponding experimental relaxation function curve with Eq. (21). The coefficients E_c, E_1, and E_2 were then approximated by empirical functions of water content using nonlinear regression analysis. The proposed correlations and the values of the parameters are presented in Table 1 with all other material properties.

3. RESULTS AND DISCUSSION

3.1. Hydro-Thermal State Simulation

Figure 4 shows the evolution of the average temperature and moisture of the grape sample obtained for drying kinetic simulated at 70°C with a relative humidity RH = 30% and an air velocity of 2.5 m/s. After the initial drying period, the evaporation was controlled by moisture diffusion rate through the product. During this period of drying, the temperature of the product was constant and approached the wet air temperature. Thereafter as the moisture flux decreased with drying time, the energy transferred to the clay product by convection became sufficient to supply heat of moisture vaporization and to heat up the product. Consequently, the product temperature increased exponentially.

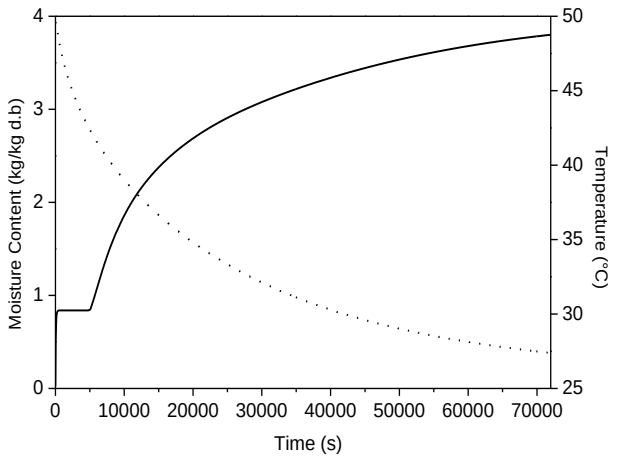

Figure 4: Variations of average moisture content and temperature of the grape versus time (T_a = 70 °C; RH = 30%; u_a = 2.5 m/s).

Figure 5 (a) shows the spatial distribution of moisture content of grape obtained at different instants of drying at 70 °C with a relative humidity of 20% and an air velocity of 2 m/s. The moisture gradient was always oriented in the same sense from the outside to the inside (r and Z) of the grape berry. However, the moisture gradient intensity changed with different sides of the studied medium. This difference is related to the considered mass transfer and corresponding surface exchange. Initially the moisture content was uniform and equal to the initial moisture content of the product. At the end of the dehydration process, the moisture tended to low moisture levels until reaching the equilibrium moisture content of the grape.

Figure 5 (b) shows the temperature distribution of the grape obtained at the same previous drying conditions (Ta = 70 °C; RH = 30%; u_a = 2.5 m/s). Unlike to the moisture gradient, the temperature gradient product was low at a specific time of the drying process. Besides, the temperature of the grape berry increased until a constant value that should correspond, in the case of convective drying, to the temperature of drying air.

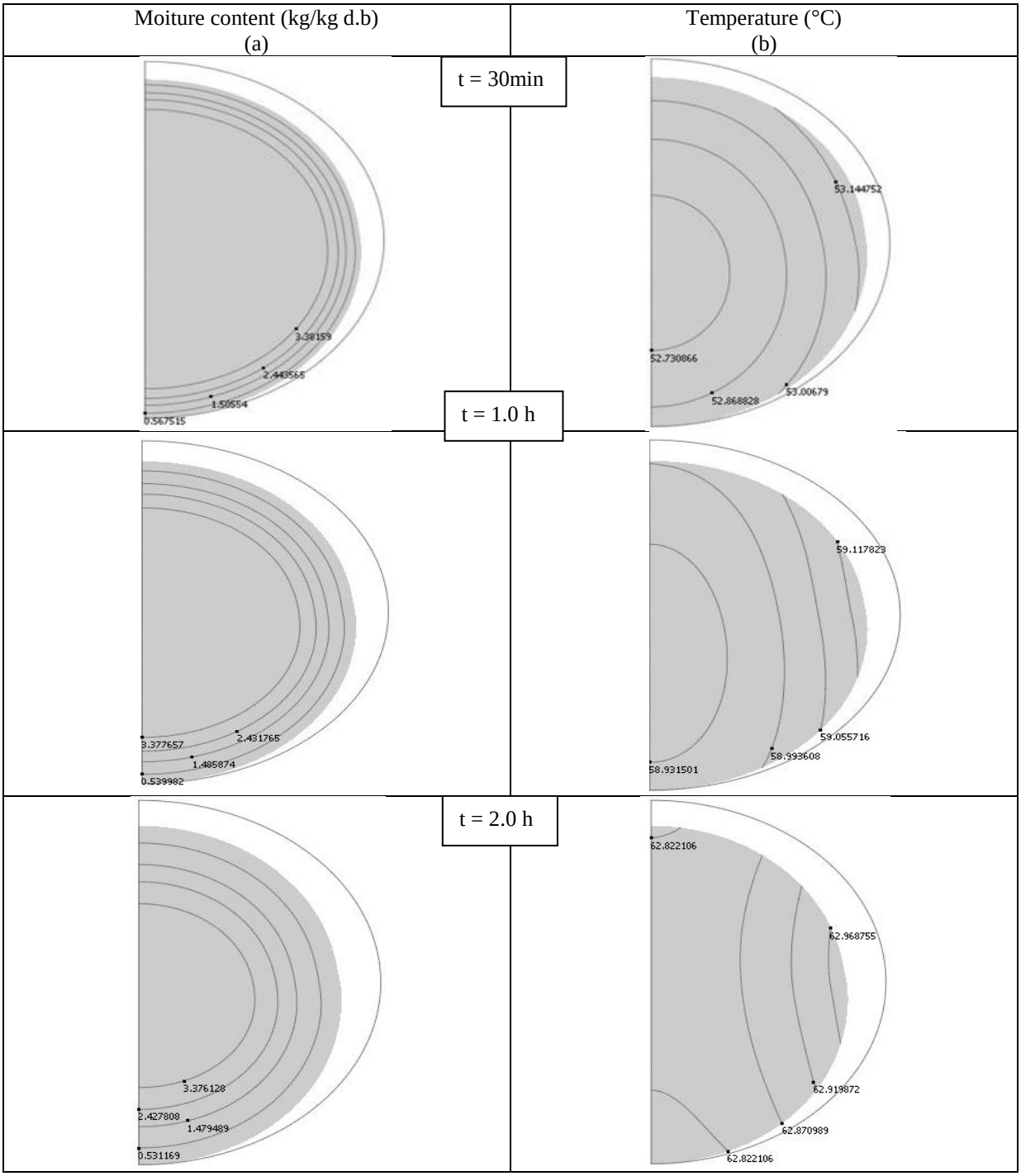

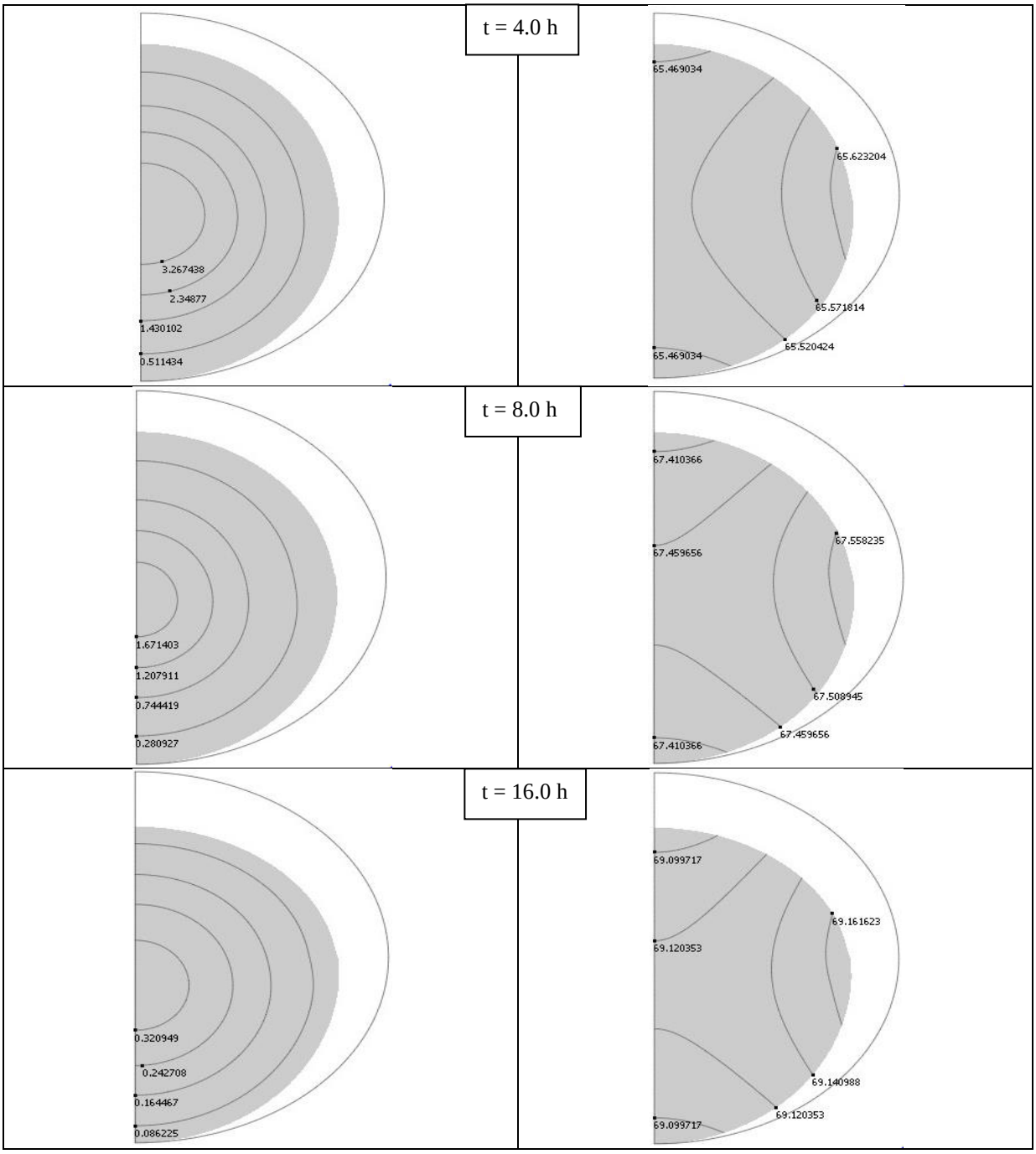

Figure 5: Moisture content and Temperature distribution within the grape at different drying times (T_a = 70 °C; RH = 30%; u_a = 2.5 m/s).

3.2. Mechanical State Simulation

The temporal evolutions of the mechanical stress in the radial direction (r) at four particular points (at the radial surface: r = 6mm, at r = 2 mm, at r = 4 mm and one in the core) are presented in Figure 6. The variation of the values of the stress between positive and negative correspond to the tensile and compressive stress. Figure 6 shows the stress level increase at the beginning of drying (because of the increase of the moisture gradient), passed by a maximum (corresponding to the beginning of the falling rate period), then decreased thereafter to reach a weak second maximum of the opposite sign and finally returned to zero, when the moisture gradient tended to zero.

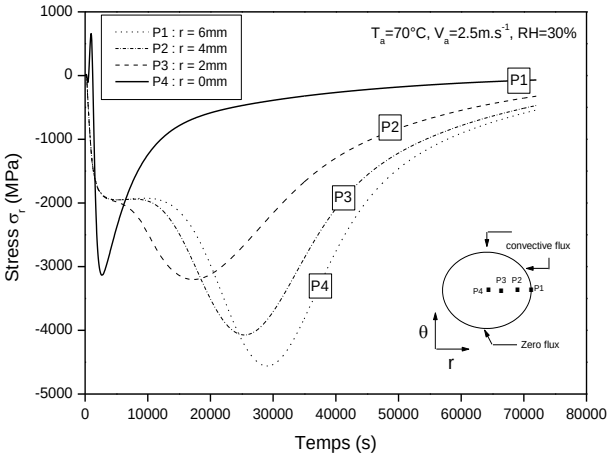

Figure 6: variation of the stresses in the r direction versus time.

In Figure 7 it can be seen at the beginning of the drying process, the superficial sample layer (in contact with hot air) was in traction while the core of the sample was in compression, as a consequence of the mechanical equilibrium. At the middle of the process, the superficial sample layer was in compression and the core of the sample was in traction, indicating that locally the stress changed its sign during the drying course. At the end of drying, the stress relaxed to zero. This phenomenon of stress reversal is specific to a viscoelastic behavior as observed by different authors [7], [13].

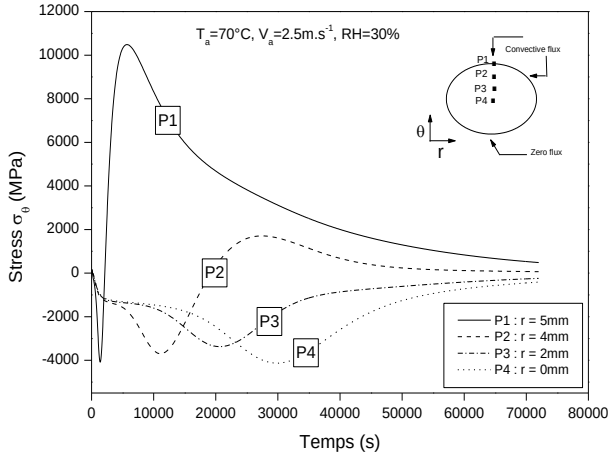

Figure 7: variation of the stresses in the Z direction versus time.

Comparing Figure 6 and Figure 7, it is noted that the maximum tensile stress was located on the sample surface in contact with air. At the beginning of drying, the r directed stress on the top surface was the strongest, but later on and until the end of drying the θ directed stress on the lateral surface was the strongest. This was due to the high hydrous shrinkage in the superficial layer and indicated that the risk of cracking caused by volume shrinkage affected mainly the radial surface. However, these cracks, if they existed, could not expand into the inner part of the sample because it was in compression.

Conclusion

A mathematical model, describing heat and mass transfers and taking into account product deformation, was suggested. The numerical solution of temperature and moisture content distributions inside the product subjected to convective drying. It is found that the temperature rises rapidly in the early drying period and as the drying process progresses, the rise of temperature attains almost steady. The moisture gradient is higher in the early drying period and as drying progresses, the moisture gradient remains almost steady. The developed model provides spatio-temporal distributions of moisture content, temperature and solid displacement within seedless grape.

References

[1] L Hassini, R Peczalski, P Laurent S Azzouz. 2-D Hydro-Viscoelastic Model for Convective Drying of Highly Deformable Saturated Product. *Drying Technology*. Volume (0), Pages 1–11, 2015.

[2] D. Mihoubi, F. Zagrouba, J. Vaxelaire, A. Bellagi, M. Roques. Transfer phenomena during the drying of shrinkable product: Modelling and simulation. *Drying Technology*, Volume 22(1–2), Pages 91–109, 2004.

[3] L.S. Arrieche, R.G. Corrêa, D.J.M. Sartori. Drying stresses and strains in a spherical food model. *Computers and Chemical Engineering*, *Volume* 33, Pages 1805–1813, 2009.

[4] S. Chemkhi, F. Zagrouba, A. Bellagi. Mathematical model for drying of highly shrinkage media. *Drying Technology* , Volume 22(5), Pages 1023–1039, 2004.

[5] M.A. Del Nobile, S. Chillo, A. Mentana, A. Baiano. Use of the generalized Maxwell model for describing the stress relaxation behavior of solid-like foods. *Journal of Food Engineering*, *Volume 78, Pages* 978–983, 2007.

[6] M.A. Rao, S.S.H. Rizvi, A. K. Datta. Engineering Properties of Food, 2nd ed.; Marcel Dekker, Inc.: New York, 1995.

[7] S.J. Kowalski. Mathematical modeling of shrinkage during drying. *Drying Technology* , Volume 14(2), Pages 307–331, 1996.

[8] P. Perré et J. Passard. A physical and mathematical model able to predict the stress field in wood over a wide range of drying conditions. *Drying Technology* , Volume 22(1–2), Pages 27–44, 2004.

[9] G. K. Vagenas, D. Marinos-Kouris, G. D. Saravacos. An analysis of mass transfer in air- drying of foods. *Drying Technology* , Volume 8(2), Pages 323–342, 1990.

[10] I. HERMASSI, S. Azzouz, L. Hassini, A. Belghith. Moisture Diffusivity of Seedless Grape undergoing convective drying, *Chemical Product and Process Modeling*, Volume (4) 1, art 1, 2017.

[11] F.D. Incropera et D.P. Dewitt. Fundamentals of heat and mass transfer. John Wiley & Sounds (Fourth Edition), 1996.

[12] K. Khalfaoui, S. Chemkhi, F. Zagrouba. Modeling and stress analysis during drying of a deformable and saturated porous medium, *Drying Technology*, Volume 31(10), Pages 1124–1137, 2013.

[13] R. Rémond, J. Passard, P. Perré. The effect of temperature and moisture content on the mechanical ehaviour of wood: A comprehensive model applied to drying and bending, *European Journal of Mechanics*, Volume (26), Pages 558–572, 2007.